Duality, inverse problems and nonlinear problems in solid mechanics

Analytical and numerical evaluation of crack-tip plasticity of an axisymmetrically loaded penny-shaped crack

Sumitra Chaiyat [a], Xiaoqing Jin [b], Leon M. Keer [b,*], Kraiwood Kiattikomol [a]

[a] *Department of Civil Engineering, King Mongkut's University of Technology, Thonburi, Bangkok 10140, Thailand*
[b] *Department of Mechanical Engineering, Northwestern University, Evanston, IL 60208, USA*

Available online 9 January 2008

Abstract

Analytical and numerical approaches are used to solve an axisymmetric crack problem with a refined Barenblatt–Dugdale approach. The analytical method utilizes potential theory in classical linear elasticity, where a suitable potential is selected for the treatment of the mixed boundary problem. The closed-form solution for the problem with constant pressure applied near the tip of a penny-shaped crack is studied to illustrate the methodology of the analysis and also to provide a fundamental solution for the numerical approach. Taking advantage of the superposition principle, an exact solution is derived to predict the extent of the plastic zone where a Tresca yield condition is imposed, which also provides a useful benchmark for the numerical study presented in the second part. For an axisymmetric crack, the numerical discretization is required only in the radial direction, which renders the programming work efficient. Through an iterative scheme, the numerical method is able to determine the size of the crack tip plasticity, which is governed by the nonlinear von Mises criterion. The relationships between the applied load and the length of the plastic zone are compared for three different yielding conditions. ***To cite this article: S. Chaiyat et al., C. R. Mecanique 336 (2008).***
© 2007 Académie des sciences. Published by Elsevier Masson SAS. All rights reserved.

Résumé

Évaluation analytique et numérique de la plasticité au voisinage du front d'une fissure en forme de pièce de monnaie soumise à un chargement axisymétrique. On utilise des approches analytiques et numériques pour résoudre un problème de fissure axisymétrique avec un modèle de Barenblatt–Dugdale raffiné. La méthode analytique utilise la théorie du potentiel en élasticité linéaire classique, un potentiel approprié étant choisi pour le traitement du problème aux limites mixte. La solution complète du problème comportant une pression uniforme appliquée au voisinage du front d'une fissure en forme de pièce de monnaie est étudiée afin d'illustrer la méthodologie de l'analyse et également fournir une solution de référence pour l'approche numérique. Grâce au principe de superposition, une solution exacte est obtenue afin de prédire l'étendue de la zone plastique où une condition de Tresca est imposée, ce qui fournit aussi un test utile pour qualifier l'étude numérique présentée dans la seconde partie. Pour une fissure axisymétrique, seule une discrétisation dans la direction radiale est requise, ce qui permet une programmation efficace. Grâce à une procédure itérative, la méthode numérique est capable d'évaluer la taille de la zone plastique, qui est déterminée par le critère non-linéaire de von Mises. Les relations entre le chargement appliqué et la taille de la zone plastique sont comparées pour trois conditions d'écoulement différentes. ***Pour citer cet article : S. Chaiyat et al., C. R. Mecanique 336 (2008).***
© 2007 Académie des sciences. Published by Elsevier Masson SAS. All rights reserved.

---

* Corresponding author.
 E-mail address: l-keer@northwestern.edu (L.M. Keer).

1. Introduction

Initiation and propagation of a fatigue crack in metallic alloys are involved with cumulative microstructural damage, as explained by Coffin [1] in terms of the plastic strain experienced locally by the material. At the microscopic level Weertman [2] has used the Bilby–Cottrell–Swinden model to study the slip zone ahead of a mode III crack. At the macroscopic level, cumulative damage theory has been examined by Fleck and Anderson [3] for varying plastic strain ranges. Knowledge of the crack tip plasticity is, therefore, fundamental for studying the failure process.

Most solid materials develop inelastic deformation when the yield strength is exceeded. Under such a circumstance, the singular stress distribution predicted by the linear elastic fracture mechanics (LEFM) becomes untenable in the region sufficiently close to the crack tip. To make the singular terms disappear, Barenblatt [4] postulated that there exists a system of cohesive forces acting near the edge of the crack, where the distance between the opposite walls of the crack is small and the molecular attractive forces become strong. He also proposed that the cohesive stresses distribute in such a manner as to cause the crack faces to close smoothly and remove the stress singularity at the crack tip.

Dugdale [5] proposed a strip-yield model to study the extent of the plastic zone in the vicinity of the crack tip. He considered a through crack of length $2l$ lying in a thin ideal elastoplastic sheet which is subjected to a uniform plane stress loading at infinity. Assuming the plastic zone is modeled as a yielded strip over some length s ahead of its two crack tips, he postulated the effect of yielding as causing an increase in the crack length that includes the extent of the plastic zone. Accordingly, the elastic–plastic crack problem is reduced to an elastic problem over a hypothetical crack of length $2(l+s)$, with the flow stress, σ_Y, applied in the yield zone to close the effective crack. Dugdale also showed good agreement between the results derived by this approach and experiment.

Since most flaws within engineering materials are more realistically represented by three dimensional (3D) geometries, it is useful to extend Dugdale's 2D hypothesis to 3D study. In this work, a penny-shaped crack of radius c is considered. When subjected to the remote axisymmetrical loading, the yield zone is assumed to occur in front of the crack tip and coplanar to the physical crack, which leads to a hypothetical penny-shaped crack of radius a. In the original 2D Dugdale approach, the requirement of the plastic zone carrying the yield stress is, in fact, equivalent to the Tresca condition, because the minimal principal stress is the stress component normal to the plane and vanishes under the plane stress condition. However, this is usually not true in 3D analysis. To address this point, the results based on the Tresca and the von Mises yielding criteria are derived in the present work and compared with those based on the original Dugdale's postulation.

The penny-shaped crack problem has received extensive investigation in the literature of fracture mechanics. One of the important solutions to the penny-shaped crack problem was derived by Sneddon [6], whose pioneer treatment by means of Hankel transform has attracted active contributions to this research field, [7–10], to name a few. Other than this popular technique, several methods are also available, such as [11,12]. The analytical method developed by Green and Zerna [13] and Collins [14] is another powerful tool. A historical review of the method and its application to axisymmetric mixed boundary value problems in elasticity is elaborated in [15]. The method was extended to study the non-axisymmetric problem by Keer [16], and its successful applications have covered various aspects of the penny-shaped crack problem [17,18].

In [18], Keer and Mura developed an analytical solutions to the penny-shaped crack under mode I loading with Tresca yield criterion prescribed in the Barenblatt–Dugdale type plastic zone. The same problem is also solved numerically by Kelly and Nowell [19] through quadratic programming. The penny-shaped crack under mixed mode loading has been studied in [20], and a related formulation for fatigue crack growth has been proposed by Chen and Keer [21]. Their work was referenced by Wang and Li [22] in developing the damage model for solids with defects

This article incorporates both an analytical method and a numerical method to investigate the plasticity zone of a penny-shaped Dugdale crack subjected to axisymmetric loading. The Green and Zerna potential as presented in [21] is employed in the analytical method. This formulation is found effective for the analytical treatment of the Tresca con-

Nomenclature

a	radius of the penny-shaped Dugdale crack	x_i	the center of the annular element along the radial direction
$A(\xi)$	unknown function in the potential		
b	outer radius of the annular ring	ϕ	Green and Zerna potential function
c	inner radius of the plastic zone	$\lambda_r^a, \lambda_r^c, \lambda_\theta^a, \lambda_\theta^c$	intermediate quantities in the expressions of the stress components
d	inner radius of the annular ring		

a　　radius of the penny-shaped Dugdale crack
$A(\xi)$　unknown function in the potential
b　　outer radius of the annular ring
c　　inner radius of the plastic zone
d　　inner radius of the annular ring
$H(x)$　Heaviside function
$J_0(\xi r), J_1(\xi r)$　Bessel function of the zeroth and the first order
K_I　mode I stress intensity factor
K_{ij}^r, K_{ij}^θ　influence coefficient of $\sigma_{rr}, \sigma_{\theta\theta}$ caused by the annular loading
l　　half length of the original two dimensional Dugdale crack
N　　number of elements used in the numerical analysis
p　　constant pressure near the crack tip
p_0　constant pressure inside the crack
$q(t)$　unknown function in $A(\xi)$
$r_0, r_1, r_i, \ldots, r_N$　discretization in the radial direction
(r, θ, z)　polar coordinates
s　　length of the plastic zone in two dimensional Dugdale crack
t　　parameter of integration
T　　uniform remote tension
u_z　displacement in z-direction

x_i　the center of the annular element along the radial direction
ϕ　Green and Zerna potential function
$\lambda_r^a, \lambda_r^c, \lambda_\theta^a, \lambda_\theta^c$　intermediate quantities in the expressions of the stress components
μ　shear modulus
ν　Poisson's ratio
σ_1, σ_3　the maximum and minimum principal stresses
$\sigma_{zz}, \sigma_{rr}, \sigma_{\theta\theta}$　normal stress components in cylindrical coordinates
$\sigma_{r\theta}, \sigma_{z\theta}, \sigma_{zr}$　shear stress components in cylindrical coordinates
$\sigma_{rr}^{(i)}, \sigma_{\theta\theta}^{(i)}$　the resultant stress components at the center of the ith element
σ_Y　yield stress of the material
τ_i　constant annular loading on the ith element
τ_j　constant annular loading on the jth element
τ_z　constant tensile loading in the annular ring
ξ　parameter of integration

Superscripts

−　　represents the reduced problem
(I)　the first part of the reduced problem
(II)　the second part of the reduced problem

dition. The detailed application of the method and some related algebraic manipulations are illustrated in Appendix A to solve the problem of the Dugdale-type yield condition. The complete solution at the crack plane is also presented for convenience of reference, since this did not appear in [21–23]. The numerical approach proposed in the second part utilizes the fundamental results shown for the solved problem in Appendix A. For the axisymmetric problem, minimal programming work is required since the discretization is only needed along the radial direction. The problem based on the Tresca criterion is linear and can be achieved in a straightforward manner. The problem based on the von Mises criterion is nonlinear; however, this mathematical difficulty can also be overcome by the present numerical computation, with the introduction of an effective iterative scheme.

2. Analytical method

2.1. Problem formulation

A three dimensional extension of Dugdale's strip yield model is considered in this study. For a penny-shaped crack of radius c under remote tension T in the z direction, a coplanar plastic yield ring is formed in front of the crack. By taking advantage of the axial symmetry, the cylindrical coordinate system (r, θ, z) is employed, as illustrated in Fig. 1. Dugdale's hypothesis approximates the size of the plastic zone by considering the enlarged crack of radius a with yielding condition satisfied in the ring . The boundary conditions are summarized as follows:

$$\sigma_{z\theta} = \sigma_{zr} = 0, \quad z = 0 \tag{1a}$$

$$u_z = 0, \quad z = 0 \; (r > a) \tag{1b}$$
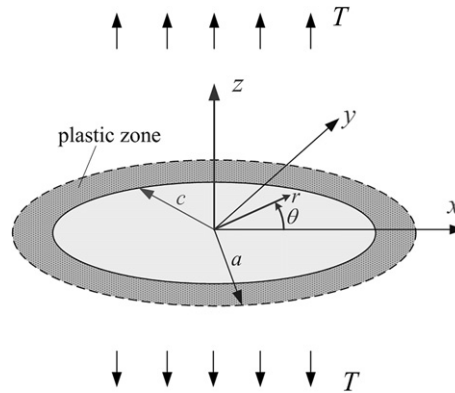
Fig. 1. Barenblatt–Dugdale type penny-shaped crack under uniform tension at infinity.

$$\sigma_{zz} = 0, \quad z = 0 \ (0 < r < c) \tag{1c}$$

$$\sigma_{zz} = T, \quad z = \infty \tag{1d}$$

$$\text{yielding condition}, \quad z = 0 \ (c < r < a) \tag{1e}$$

In the last of the above boundary conditions, i.e. Eq. (1e), three types of yielding conditions are of current interest:

(1) the original Dugdale's condition postulates,

$$\sigma_{zz} = \sigma_Y, \quad z = 0 \ (c < r < a) \tag{2a}$$

where σ_Y is the yield stress of the material subject to uniaxial tension. The solution to this problem is discussed in Appendix A and in Maugis [23].
(2) Tresca's yield condition gives

$$|\sigma_1 - \sigma_3| = \sigma_Y, \quad z = 0 \ (c < r < a) \tag{2b}$$

where σ_1 and σ_3 are the maximum and minimum principal stresses. For comparison, this problem is solved both analytically and numerically in the current study.
(3) von Mises criterion for the current problem may be expressed as

$$(\sigma_{zz} - \sigma_{rr})^2 + (\sigma_{zz} - \sigma_{\theta\theta})^2 + (\sigma_{rr} - \sigma_{\theta\theta})^2 = 2\sigma_Y^2, \quad z = 0 \ (c < r < a) \tag{2c}$$

where the problem is solved numerically.

According to Green and Zerna [13], the solution to an axisymmetric problem may be expressed by a potential function ϕ,

$$\sigma_{zz} = -\frac{\partial^2 \phi}{\partial z^2} + z\frac{\partial^3 \phi}{\partial z^3} \tag{3a}$$

$$\sigma_{\theta\theta} = -\frac{\partial^2 \phi}{\partial z^2} - (1 - 2\nu)\frac{\partial^2 \phi}{\partial r^2} + \frac{z}{r}\frac{\partial^2 \phi}{\partial z\partial r} \tag{3b}$$

$$\sigma_{rr} = \frac{\partial^2 \phi}{\partial r^2} + \frac{2\nu}{r}\frac{\partial \phi}{\partial r} + z\frac{\partial^3 \phi}{\partial z\partial r} \tag{3c}$$

$$\sigma_{zr} = z\frac{\partial^3 \phi}{\partial z^2\partial r} \tag{3d}$$

$$\sigma_{z\theta} = \frac{z}{r}\frac{\partial^3 \phi}{\partial z^2\partial \theta} \tag{3e}$$

$$2\mu u_z = -2(1 - \nu)\frac{\partial \phi}{\partial z} + z\frac{\partial^2 \phi}{\partial z^2} \tag{3f}$$

where μ and ν are the shear modulus and Poisson's ratio of the material, respectively.

A suitable form for the potential function ϕ can be expressed as [21]

$$\phi = -\int_0^\infty \frac{1}{\xi} A(\xi) e^{-\xi z} J_0(\xi r) \, d\xi \tag{4}$$

where $J_0(\xi r)$ is the zeroth order Bessel function and $A(\xi)$ is an unknown function determined from the boundary conditions. By using the potential function of Eqs. (3), (4), it is seen that the boundary condition (1a) is automatically satisfied. To reconcile the unsatisfactory boundary condition (1d), a reduced problem is considered, which is formulized through the superposition principle.

2.2. Solution to the problem with Tresca yielding condition

Assuming the Tresca yield condition is satisfied in the domain of plastic ring $c < r < a$, the boundary conditions (Eqs. (1a)–(1d)) are still valid in this case, while the last condition (Eq. (1e)) takes the form of Eq. (2b). It is assumed at this stage that the maximum principal stress in the plastic zone is σ_{zz} and the minimum principal stress is $\sigma_{\theta\theta}$, Eq. (2b) is thus

$$\sigma_{zz} - \sigma_{\theta\theta} = \sigma_Y, \quad z = 0 \ (c < r < a) \tag{5}$$

The justification of the above assumption will be checked, a posteriori, after the solution is obtained.

According to the principle of superposition, the above problem may be reduced after subtracting a uniaxial uniform stress of $\sigma_{zz}^{(0)} = T$ whereby all other stress components vanish. For the reduced problem, the first two boundary conditions are Eqs. (1a), (1b), while the last three boundary conditions become [18]

$$\bar{\sigma}_{zz} = -T, \quad z = 0 \ (0 < r < c) \tag{6c}$$

$$\bar{\sigma}_{zz} = 0, \quad z = \infty \tag{6d}$$

$$\bar{\sigma}_{zz} - \bar{\sigma}_{\theta\theta} = \sigma_Y - T, \quad z = 0 \ (c < r < a) \tag{6e}$$

where σ_{zz} with the symbol 'bar' on represents the modified stress component in the reduced problem. The principle of superposition may be employed again to further simplify the algebra involved in the above reduced problem, which is decomposed as the summation of the following two problems. The first problem corresponds to the penny-shaped crack under uniform internal load $-T$ inside the crack, which is solved in Appendix A. From Eqs. (A.21)–(A.23), the stress components inside the crack ($r < a$) for the first problem are

$$\bar{\sigma}_{zz}^{(I)} = -T \tag{7a}$$

$$\bar{\sigma}_{\theta\theta}^{(I)} = -T\left(\frac{1}{2} + \nu\right) \tag{7b}$$

$$\bar{\sigma}_{rr}^{(I)} = -T\left(\frac{1}{2} + \nu\right) \tag{7c}$$

where the superscript [I] represents the first part of the reduced problem. Accordingly, the corresponding boundary conditions (Eqs. (6c)–(6e)) are adapted for the second problem as

$$\bar{\sigma}_{zz}^{(II)} = 0, \quad z = 0 \ (0 < r < c) \tag{8c}$$

$$\bar{\sigma}_{zz}^{(II)} = 0, \quad z = \infty \tag{8d}$$

$$\bar{\sigma}_{zz}^{(II)} - \bar{\sigma}_{\theta\theta}^{(II)} = \sigma_Y - T\left(\frac{1}{2} + \nu\right), \quad z = 0 \ (c < r < a) \tag{8e}$$

where the superscript [II] represents the second part of the reduced problem. This problem may also be solved by the method given in Appendix A. First, using the Green–Zerna potential, Eq. (8e) leads to

$$(1 - 2\nu)\frac{\partial^2 \phi}{\partial r^2}\bigg|_{z=0} = \sigma_Y - \left(\frac{1}{2} + \nu\right)T \tag{9}$$

Utilizing Eq. (A.9), the above Eq. (9) yields

$$\frac{d}{dr}\left[\frac{1}{r}\int_c^r \frac{tq(t)}{\sqrt{r^2-t^2}}\,dt\right] = \frac{2\sigma_Y - (1+2\nu)T}{2(1-2\nu)} \tag{10}$$

The solution to the above Abel type integral equation is determined as

$$q(t) = \frac{2}{\pi}\frac{2\sigma_Y - (1+2\nu)T}{(1-2\nu)}\left[\sqrt{t^2-c^2} - \frac{c}{2}\cos^{-1}(c/t)\right] \tag{11}$$

Compared with the above result, there appears to be a misprint in the solution given in [18]. In the plastic zone, the stress components are evaluated as follows:

$$\bar{\sigma}_{zz}^{(II)} = \frac{2\sigma_Y - (1+2\nu)T}{2(1-2\nu)}\left(2 - \frac{c}{r}\right)$$

$$\bar{\sigma}_{\theta\theta}^{(II)} = \frac{2\sigma_Y - (1+2\nu)T}{2(1-2\nu)}\left(1 - \frac{c}{r} + 2\nu\right)$$

$$\bar{\sigma}_{rr}^{(II)} = \frac{2\sigma_Y - (1+2\nu)T}{2(1-2\nu)}\left(1 - 2\nu\frac{c}{r} + 2\nu\right) \tag{12}$$

After carrying out the superposition, the following results are arrived for the penny-shaped Dugdale crack with Tresca condition prescribed in the yield ring:

$$\sigma_{zz} - \sigma_{zz} = \sigma_Y$$

$$\sigma_{zz} - \sigma_{rr} = \sigma_Y - \left[\sigma_Y - \left(\frac{1}{2}+\nu\right)T\right]\frac{c}{r}$$

$$\sigma_{rr} - \sigma_{\theta\theta} = \left[\sigma_Y - \left(\frac{1}{2}+\nu\right)T\right]\frac{c}{r} \tag{13}$$

Since c/r in plastic domain is smaller than 1, it is now seen that Tresca's yield criterion given by Eq. (5) is valid.

The requirement that the stress singularity vanishes at $r = a$ gives the relationship between the applied stress and the length of the plastic zone

$$\frac{(1-2\nu)T/\sigma_Y}{2 - (1+2\nu)T/\sigma_Y} = \sqrt{1 - (c/a)^2} - \frac{c}{2a}\cos^{-1}(c/a) \tag{14}$$

which verifies Keer and Mura's result [18]. Using the above results, one may also evaluate the stress components for $r > a$ on the crack plane $z = 0$. From those lengthy expressions, whose details are not transcribed here, two interesting results are observed. The singularities of $\sigma_{\theta\theta}$ and σ_{rr} at $r = a$ also vanish as the condition (14) is satisfied. In such an instance, the stress components σ_{zz}, $\sigma_{\theta\theta}$ and σ_{rr} all exhibit continuous distribution on the crack plane $z = 0$.

3. Numerical method

In this section, a numerical approach is proposed to solve the axisymmetric crack problem. The fundamentals of the numerical method are based on the solution of a penny-shaped crack under constant annular loading inside the crack, which may be readily deduced from the analytical solution of the problem solved in Appendix A. Both of the problems considering Tresca and von Mises criterion are solved by employing this numerical technique.

3.1. Formulation and discretization

Consider a penny-shaped crack of radius a subject to a constant annular ($d < r < b$) tensile stress τ_z, as shown in Fig. 2. The solution to this problem may be deduced from the problem solved in Appendix A through superposition, noting the difference of the sign convention. The following induced stresses in zones (i)–(iii) along the crack face are derived.
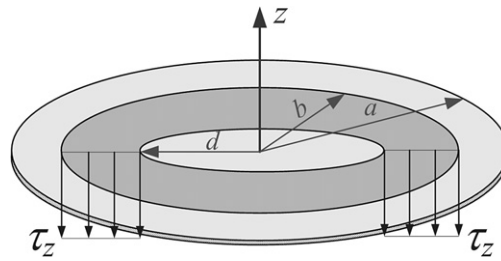
Fig. 2. Penny-shaped crack of radius a subject to a constant annular ($d < r < b$) tensile stress τ_z on the crack face.

- Zone (i) ($r < d$, $z = 0$):

$$\sigma_{zz} = \sigma_{\theta\theta} = \sigma_{rr} = 0 \tag{15}$$

- Zone (ii) ($d < r < b$, $z = 0$):

$$\sigma_{zz} = \tau_z$$
$$\sigma_{\theta\theta} = \tau_z\left[\left(\frac{1}{2} + \nu\right) - \left(\frac{1}{2} - \nu\right)\frac{d^2}{r^2}\right]$$
$$\sigma_{rr} = \tau_z\left[\left(\frac{1}{2} + \nu\right) + \left(\frac{1}{2} - \nu\right)\frac{d^2}{r^2}\right] \tag{16}$$

- Zone (iii) ($b < r < a$, $z = 0$):

$$\sigma_{zz} = 0$$
$$\sigma_{\theta\theta} = \tau_z\left[\left(\frac{1}{2} - \nu\right)\frac{(b^2 - d^2)}{r^2}\right]$$
$$\sigma_{rr} = -\tau_z\left[\left(\frac{1}{2} - \nu\right)\frac{(b^2 - d^2)}{r^2}\right] \tag{17}$$

The stress intensity factor (SIF) at $r = a$ due to the annular loading is given by

$$K_{\mathrm{I}} = \frac{2\tau_z}{\sqrt{\pi a}}\left(\sqrt{a^2 - b^2} - \sqrt{a^2 - d^2}\right) \tag{18}$$

In the numerical solution, the stress component σ_{zz} on the crack face is regarded as unknown. The axisymmetric distribution of σ_{zz} on $z = 0$, $r < a$ may be discretized on the annulus. The discretization is only required along the radial direction, while it is also noted that this radial discretization can be non-uniform.

In the radial direction, the penny-shaped crack is discretized into N elements. On each element, the stress σ_{zz} is assumed to be constant. Although this may lead to some error, however, when the total number of the elements becomes larger and the size of each element becomes sufficiently small, reasonable accuracy can be achieved. Other stress components $\sigma_{\theta\theta}$ and σ_{rr} may also occur due to the existence of σ_{zz} in each annual ring to ensure an equilibrium of the stress state, as demonstrated by Eqs. (16), (17). The resultant stress components can therefore be calculated by superposing the contributions from all the annular elements.

3.2. Case study

3.2.1. The Tresca criterion

The penny-shaped crack is first discretized as described in the previous section. The non-zero σ_{zz} exists only in the yield zone ($c < r < a$), which is the computational domain to be discretized in the current computation. Assuming N elements are used in this analysis, the yield zone is discretized along the radial direction, $c = r_0 < r_1 < r_2 < \cdots < r_N = a$, as shown in Fig. 3. The magnitude of σ_{zz} on the jth element is assumed to be τ_j, which is the unknown that
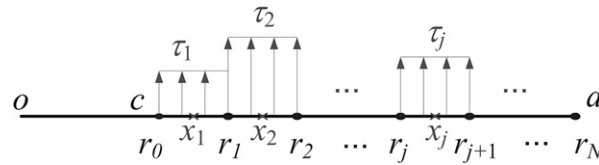
Fig. 3. Discretization of the plastic zone ($c < r < a$) along the radial direction.

needs to be determined. The Tresca yield condition is made to be satisfied at the center of each element. Denote x_i as the center of the ith element

$$x_i = \frac{1}{2}(r_i + r_{i-1}) \tag{19}$$

The induced stress $\sigma_{\theta\theta}$ at x_i can be determined from Eqs. (15)–(17), with r replaced by x_i. This relation is recorded in the following form:

$$\sigma_{\theta\theta}(r = x_i) = \sum_{j=1}^{N} K_{ij}^{\theta} \tau_j \tag{20}$$

where the influence coefficient, K_{ij}^{θ}, can be determined accordingly from either of the Eqs. (15)–(17).

The uniform remote tension T may be regarded as an additional unknown. From the result in Appendix A, it is seen that T also causes $\sigma_{\theta\theta}$ on the crack face, although with no effect on σ_{zz}, i.e.,

$$\sigma_{\theta\theta}(r = x_i) = -T\left(\frac{1}{2} + \nu\right) \tag{21}$$

Summarizing all the contributions, the Tresca's condition at x_i gives

$$\left(\frac{1}{2} + \nu\right)T + \tau_i - \sum_{j=1}^{N} K_{ij}^{\theta} \tau_j = \sigma_Y \quad (i = 1, 2, \ldots, N) \tag{22}$$

The above equation gives a total of N linear algebraic equations, while a total of $N + 1$ unknowns is present in the current problem. The additional equation is derived by considering that the SIF vanishes at $r = a$, which may be formulated by considering the contributions to the SIFs from T and each τ_j, cf. Eqs. (18) and (A.24),

$$2T\sqrt{\frac{a}{\pi}} - \frac{2}{\sqrt{\pi a}} \sum_{j=1}^{N} \left[\left(\sqrt{a^2 - r_{j-1}^2} - \sqrt{a^2 - r_j^2}\right)\tau_j\right] = 0 \tag{23}$$

From Eqs. (22) and (23), a system of $N + 1$ linear algebraic equations with a total of $N + 1$ unknowns is formulated. The unknowns in Eqs. (22) and (23) may be nondimensionalized by σ_Y. After solving the system of linear algebraic equations, the numerical results for T/σ_Y and τ_j/σ_Y $(j = 1, 2, \ldots, n)$ are obtained.

3.2.2. The von Mises criterion

The discretization for the von Mises criterion problem is the same as in the preceding. It is noted that Eqs. (19)–(21), (23) of the previous section remain valid for the current problem. The resultant $\sigma_{\theta\theta}$ at $r = x_i$ is denoted as

$$\sigma_{\theta\theta}^{(i)} = -T\left(\frac{1}{2} + \nu\right) + \sum_{j=1}^{N} K_{ij}^{\theta} \tau_j \tag{24}$$

Similar to Eqs. (19), (20), the resulting stress σ_{rr} on the crack face is found by utilizing Eqs. (25) and (26) where

$$\sigma_{rr}(r = x_i) = \sum_{j=1}^{N} K_{ij}^{r} \tau_j \tag{25}$$

due to the annular tensile loading τ_j, where the influence coefficient, K_{ij}^r, is determined from either of Eqs. (15)–(17), and

$$\sigma_{rr}(r = x_i) = -T\left(\frac{1}{2} + \nu\right) \tag{26}$$

due to the uniform remote tension T. Consequently, the resultant σ_{rr} at $r = x_i$ is

$$\sigma_{rr}^{(i)} = -T\left(\frac{1}{2} + \nu\right) + \sum_{j=1}^{N} K_{ij}^r \tau_j \tag{27}$$

Enforcing the von Mises criterion, i.e. Eq. (2c), at x_i gives

$$\left(\tau_i - \sigma_{\theta\theta}^{(i)}\right)^2 + \left(\tau_i - \sigma_{rr}^{(i)}\right)^2 + \left(\sigma_{rr}^{(i)} - \sigma_{\theta\theta}^{(i)}\right)^2 = 2\sigma_Y^2 \quad (i = 1, 2, \ldots, N) \tag{28}$$

Eq. (28) essentially is a system of nonlinear algebraic equations, which, however, cannot be solved in a straightforward manner as experienced in the previous case. An iterative scheme is employed to facilitate the programming. First, the above Eq. (28) is reorganized as follows:

$$\tau_i = \sigma_{\theta\theta}^{(i)} + \sqrt{2\sigma_Y^2 - \left(\tau_i - \sigma_{rr}^{(i)}\right)^2 - \left(\sigma_{rr}^{(i)} - \sigma_{\theta\theta}^{(i)}\right)^2} \quad (i = 1, 2, \ldots, N) \tag{29}$$

It is implicitly assumed above that $\tau_i \geqslant \sigma_{\theta\theta}^{(i)}$ holds in the plastic zone. This assumption is instantly verified once a convergent solution is established. Next, the right-hand side of Eq. (29) is evaluated by the known value from the previous iteration step, and its result is used to update the value of τ_i for the current iteration step. Finally, with the current value of τ_i, Eq. (23) is used to update the remote tension T. In this study, the initial values for τ_i are set as zeros, and the above iteration is repeated until satisfactory convergence is attained, i.e., the maximum difference between the current and the previous values of τ_i is controlled within a given tolerance. Numerical examples show that the proposed iterative scheme is quite efficient. In some cases, the relative error between two successive iterations converges to 10^{-8} after about 10 iterations.

4. Results and discussions

For the plastic zone governed by the Tresca criterion, Eq. (14) shows its length is dependent on Poisson's ratio, which differs from a Dugdale crack, as given by Eq. (A.27). Fig. 4 shows the influence of Poisson's ratio on the length of the plastic zone. The analytical results for various Poisson's ratios are compared with the results of a penny-shaped Dugdale crack. The comparison shows that as the applied load becomes larger, the results based on Dugdale's condition approach the Tresca condition with higher Poisson's ratios. It is also observed that as the Poisson's ratio increases, the applied stress must increase to acquire the same length of plastic zone. This coincides qualitatively with the crack tip plastic zone result for a 2D semi-infinite crack [24]. Considering the particular case when the Poisson's ratio reaches 0.5, it is recognized from Eq. (14) that $a/c = 1$ and hence no plastic zone can occur when the applied tension T is below the yield stress.
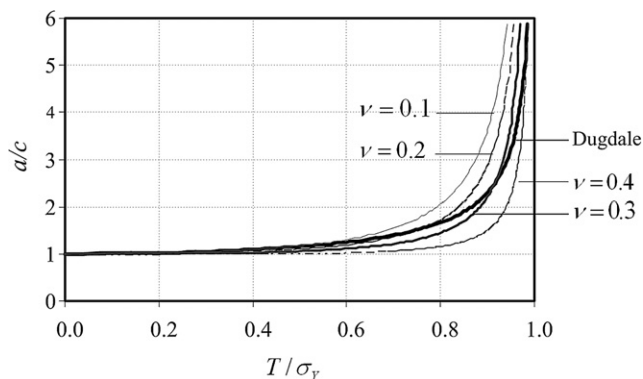

Fig. 4. Comparison of the analytical results of the Dugdale condition and the Tresca condition with various Poisson's ratios.
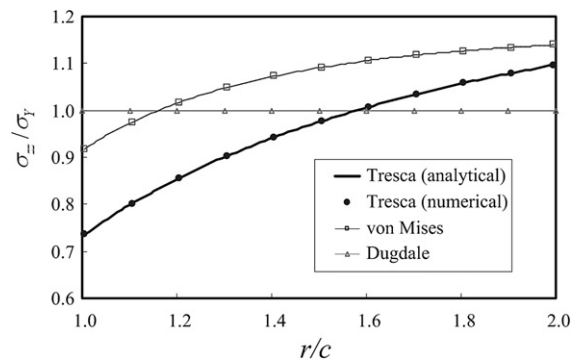
Table 1
Convergence of the numerical results based on the von Mises condition with various element numbers ($\nu = 0.25$)

N	$a/c = 1.05$		$a/c = 2.0$		$a/c = 6.0$	
	Iterations	CPU time (s)	Iterations	CPU time (s)	Iterations	CPU time (s)
50	11	0.031	50	0.047	299	0.203
100	11	0.063	50	0.125	299	0.672
200	11	0.250	50	0.594	299	2.531
500	11	3.484	50	5.547	299	17.563
1000	11	24.781	50	32.625	299	81.547

Table 2
Convergence of the numerical results based on the von Mises condition for various Poisson's ratios ($N = 100$)

ν	$a/c = 1.05$		$a/c = 2.0$		$a/c = 6.0$	
	Iterations	CPU time (s)	Iterations	CPU time (s)	Iterations	CPU time (s)
0.20	11	0.047	50	0.016	299	0.172
0.25	11	0.016	49	0.047	328	0.172
0.30	17	0.031	49	0.016	364	0.172
0.40	46	0.031	61	0.047	467	0.297
0.45	103	0.078	121	0.078	543	0.313

Fig. 5. Variation of the normalized σ_{zz} in the plastic zone for the three different yield conditions.

The convergence of the numerical results based on the von Mises condition is presented in Tables 1 and 2. In the computation, the result is considered as convergent when the maximum absolute error between two successive iterations is below 10^{-8}. As shown in Table 1, the grid size virtually has no effect on the total number of iterations required to achieve a convergent results. However, the computational time usually increases in a nonlinear manner when more elements are used (Table 1). For $\nu = 0.25$, the iteration usually converges in less than 300 loops when a/c is smaller than 6. It is also found that the convergence of the numerical computation does depend on the Poisson's ratio, and usually larger value of ν decreases the convergent speed (Table 2). It takes less than 1 second to run a typical problem on a Pentium 4 computer, when 100 elements are used.

The distribution of the normalized σ_{zz} in the yielding zone is shown in Fig. 5 for the three yield conditions when $a/c = 2$ and $\nu = 0.25$. For the Tresca condition, the maximum relative error between the numerical and analytical solutions is about 4×10^{-5}, when 100 elements are used in the discretization. The comparison of all the three yield conditions for $\nu = 0.25$ is shown in Fig. 6, where the analytical results based on the Tresca yield condition are provided to benchmark the present numerical analysis. Here, 100 elements are employed for the numerical results of both the Tresca and von Mises criterions. For the Tresca condition, it is difficult to discern the difference between the numerical and the analytical results in the figure, since the absolute error of the numerical method is generally about 10^{-5} (Table 3).

It is postulated in [18] that the von Mises criterion might be more reasonable to decide the plastic domain. As a calibration, the results based on the Dugdale condition and the Tresca criterion are compared with the von Mises
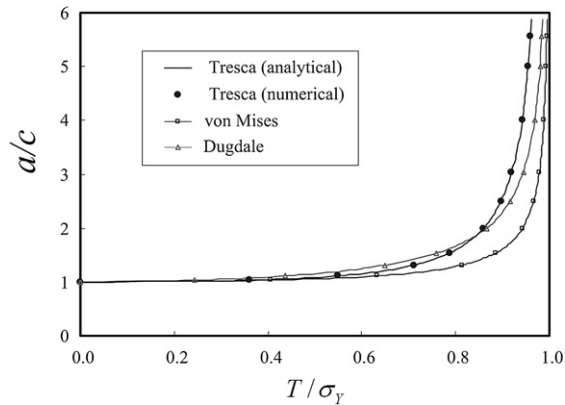
Fig. 6. Comparison of three different yielding conditions for small a/c and $\nu = 0.25$.

Table 3
The numerical results vs. the analytical results of the Tresca condition for $\nu = 0.25$

a/c	T/σ_Y		
	Analytical	Numerical	Absolute error
1.2	0.6411261	0.6411176	0.0000085
1.6	0.8004665	0.8004542	0.0000122
2.0	0.8592893	0.8592767	0.0000126
4.0	0.9423774	0.9423733	0.0000041
6.0	0.9637025	0.9637034	0.0000008

Table 4
Comparison of numerical results of the three yielding conditions for small a/c and $\nu = 0.25$

a/c	T/σ_Y		
	Tresca	Von Mises	Dugdale
1.02	0.307274	0.33987659	0.1970564
1.04	0.396142	0.44732872	0.2746703
1.06	0.454172	0.51818407	0.3316678
1.08	0.497475	0.57088019	0.3777051
1.10	0.531968	0.61246836	0.4165978
1.12	0.560549	0.64650576	0.4503399

condition. It is observed in Fig. 6 that the plastic zone based on the von Mises criterion usually possesses a shorter length than the other two criteria. It is also indicated that when the yield zone is small ($a/c \sim 1$), the Dugdale condition gives the longest length of the plastic zone (Table 4). However, as the yield zone becomes larger ($a/c > 3$), the prediction based on Dugdale condition lies between the results based on the other two criteria.

5. Conclusions

This article discusses both analytical and numerical solutions of an axisymmetric penny-shaped crack. Using the Barenblatt–Dugdale model, the crack tip plasticity is investigated for three types of yield conditions. The numerical solution to the problem with a Tresca yield condition is benchmarked by the derived analytical solution, which shows reasonable agreement. The proposed numerical method is effective and the programming implementation is convenient, as demonstrated in solving the nonlinear problem with the von Mises criterion.

Acknowledgements

Appendix A. Solution to the problem of Dugdale type yielding condition

A.1. Constant pressure near the crack tip

For a pressurized crack with constant pressure p on $c < r < a$ and zero on $r < c$, assuming the penny-shaped crack of radius a is contained in an infinite media devoid of external loading, the first three boundary conditions, Eqs. (1a)–(1c), are retained, while the last two, Eqs. (1d) and (1e), need to be replaced by the following:

$$\sigma_{zz} = 0, \quad z = \infty \tag{A.1d}$$

$$\sigma_{zz} = -p, \quad z = 0 \ (c < r < a) \tag{A.1e}$$

It is seen that the boundary condition (A.1d) is automatically satisfied by the potential of Eq. (4). For the current problem, the function is chosen as

$$A(\xi) = \int_c^a q(t) \sin(\xi t)\, dt \tag{A.2}$$

with the restriction to ensure that no stress singularity occurs at $r = c$

$$q(c) = 0 \tag{A.3}$$

With the assistance of the identity

$$\int_0^\infty \sin(\xi t) J_0(\xi r)\, d\xi = \frac{H(t - r)}{\sqrt{t^2 - r^2}} \tag{A.4}$$

the following result is obtained after interchanging the sequence of integration:

$$\left. \frac{\partial \phi}{\partial z} \right|_{z=0} = \int_c^a q(t) \frac{H(t - r)}{\sqrt{t^2 - r^2}}\, dt \tag{A.5}$$

where $H(x)$ is the Heaviside function, with

$$H(x) = \begin{cases} 1 & (x \geqslant 0) \\ 0 & (x < 0) \end{cases} \tag{A.6}$$

Similarly, by utilizing the identities

$$\frac{d J_0(\xi r)}{d r} = -\xi J_1(\xi r) \tag{A.7}$$

where $J_1(\xi r)$ is the Bessel function of the first order, and

$$\int_0^\infty \sin(\xi t) J_1(\xi r)\, d\xi = \frac{t}{r\sqrt{r^2 - t^2}} H(r - t) \tag{A.8}$$

the following result is derived:

$$\left. \frac{\partial \phi}{\partial r} \right|_{z=0} = \int_c^a \frac{t q(t)}{r\sqrt{r^2 - t^2}} H(r - t)\, dt \tag{A.9}$$

From Eq. (4),

$$\frac{\partial^2 \phi}{\partial z^2} = -\int_0^\infty \xi A(\xi) e^{-\xi z} J_0(\xi r)\, dr \tag{A.10}$$

Owing to the condition (A.3), $A(\xi)$ may be rewritten in the following form after carrying out integration by parts

$$A(\xi) = -q(a)\frac{\cos(\xi a)}{\xi} + \frac{1}{\xi}\int_c^a \cos(\xi t) q'(t)\, dt \tag{A.11}$$

Substituting (A.11) to (A.10) and using the identity

$$\int_0^\infty \cos(\xi t) J_0(\xi r)\, d\xi = \frac{H(r-t)}{\sqrt{r^2 - t^2}} \tag{A.12}$$

the following result is achieved:

$$\left.\frac{\partial^2 \phi}{\partial z^2}\right|_{z=0} = q(a)\frac{H(r-a)}{\sqrt{r^2 - a^2}} - \int_c^a q'(t)\frac{H(r-t)}{\sqrt{r^2 - t^2}}\, dt \tag{A.13}$$

Now it is seen from Eqs. (3f) and (A.5), boundary condition (1b) is automatically satisfied, and from Eqs. (3a) and (A.13), boundary condition (1c) is also automatically satisfied. The only remaining boundary condition (A.1e) leads to

$$\int_c^r \frac{q'(t)}{\sqrt{r^2 - t^2}}\, dt = -p \tag{A.14}$$

After inverting the above Abel integral equation, the following solution is determined with the requirement of (A.3),

$$q(t) = -\frac{2}{\pi} p\sqrt{t^2 - c^2} \tag{A.15}$$

Substituting this result into Eqs. (A.2), (4), and (3a)–(3c), one may obtain the stress distribution on the crack plane $z = 0$. It is found that all the stress components vanish for $r < c$. When $r > c$, the nonvanishing stress components are

$$\sigma_{zz} = \begin{cases} -p, & c < r < a \\ \dfrac{2}{\pi} p\left[\sqrt{\dfrac{a^2 - c^2}{r^2 - a^2}} - \sin^{-1}\sqrt{\dfrac{a^2 - c^2}{r^2 - c^2}}\right], & r > a \end{cases} \tag{A.16}$$

$$\sigma_{\theta\theta} = \begin{cases} -p\lambda_\theta^c, & c < r < a \\ \dfrac{2}{\pi} p\left(\lambda_\theta^a\sqrt{\dfrac{a^2 - c^2}{r^2 - a^2}} - \lambda_\theta^c \sin^{-1}\sqrt{\dfrac{a^2 - c^2}{r^2 - c^2}}\right), & r > a \end{cases} \tag{A.17}$$

$$\sigma_{rr} = \begin{cases} -p\lambda_r^c, & c < r < a \\ \dfrac{2}{\pi} p\left(\lambda_r^a\sqrt{\dfrac{a^2 - c^2}{r^2 - a^2}} - \lambda_r^c \sin^{-1}\sqrt{\dfrac{a^2 - c^2}{r^2 - c^2}}\right), & r > a \end{cases} \tag{A.18}$$

where in the above Eqs. (A.17), (A.18),

$$\begin{aligned} \lambda_\theta^c &= \left(\frac{1}{2} + v\right) - \left(\frac{1}{2} - v\right)\frac{c^2}{r^2}, & \lambda_\theta^a &= \left(\frac{1}{2} + v\right) - \left(\frac{1}{2} - v\right)\frac{a^2}{r^2} \\ \lambda_r^c &= \left(\frac{1}{2} + v\right) + \left(\frac{1}{2} - v\right)\frac{c^2}{r^2}, & \lambda_r^a &= \left(\frac{1}{2} + v\right) + \left(\frac{1}{2} - v\right)\frac{a^2}{r^2} \end{aligned} \tag{A.19}$$

The mode I stress intensity factor is determined from Eq. (A.16),

$$K_I = \lim_{r \to a^+} \sqrt{2\pi(r-a)}\sigma_{zz} = \frac{2p}{\sqrt{\pi a}}\sqrt{a^2 - c^2} \tag{A.20}$$

The displacement inside the crack is found from Eqs. (A.15), (A.5) and (3f)

$$u_z = \frac{2(1-\nu)}{\pi\mu}p\int\limits_{\max(r,c)}^{a}\sqrt{\frac{t^2 - c^2}{t^2 - r^2}}\,dt \quad (z = 0,\ r < a) \tag{A.21}$$

The integral in the above equation may be expressed as functions of elliptic integrals, whose details are given in [23].

A.2. Constant pressure inside the crack

A special yet important case is that when constant pressure p_0 is applied inside the entire crack. The solution to this problem can be readily deduced by substituting $c = 0$ into the above results of the previous section, which yields

$$\sigma_{zz} = \begin{cases} -p_0, & r < a \\ \dfrac{2}{\pi}p_0\left[\dfrac{a}{\sqrt{r^2 - a^2}} - \sin^{-1}(a/r)\right], & r > a \end{cases} \tag{A.22}$$

$$\sigma_{\theta\theta} = \begin{cases} -p_0\left(\dfrac{1}{2} + \nu\right), & r < a \\ \dfrac{2}{\pi}p_0\left[\lambda_\theta^a\dfrac{a}{\sqrt{r^2 - a^2}} - \left(\dfrac{1}{2} + \nu\right)\sin^{-1}(a/r)\right], & r > a \end{cases} \tag{A.23}$$

$$\sigma_{rr} = \begin{cases} -p_0\left(\dfrac{1}{2} + \nu\right), & r < a \\ \dfrac{2}{\pi}p_0\left[\lambda_r^a\dfrac{a}{\sqrt{r^2 - a^2}} - \left(\dfrac{1}{2} + \nu\right)\sin^{-1}(a/r)\right], & r > a \end{cases} \tag{A.24}$$

where λ_θ^a and λ_r^a in the above Eqs. (A.23), (A.24) are given by Eq. (A.19).

The mode I stress intensity factor is

$$K_I = \frac{2}{\pi}p_0\sqrt{\pi a} \tag{A.25}$$

The problem of a penny-shaped crack under remote tension which is uniformly applied at infinity can be reduced to the above pressurized crack problem, according to the superposition principle.

A.3. Penny-shaped Dugdale crack

When the uniform tension T is applied at infinity, a ring-shaped plastic zone is accumulated in the region, $c < r < a$, where a closure stress equal to σ_Y is applied to remove the singularity at the crack tip $r = a$. To simplify the calculation, the problem is handled by superposing two solutions: a penny-shaped crack under remote tension T, whose SIF can be deduced by Eq. (A.25), and a penny-shaped crack under constant closure stress of Eq. (2a) at the tip, whose SIF can be determined by (A.20). The SIF for the resultant problem must vanish, therefore,

$$\frac{2}{\pi}T\sqrt{\pi a} - \frac{2\sigma_Y}{\sqrt{\pi a}}\sqrt{a^2 - c^2} = 0 \tag{A.26}$$

From the above equation, the relationship between the length of the plastic zone and the applied load is determined:

$$\frac{T}{\sigma_Y} = \sqrt{1 - \left(\frac{c}{a}\right)^2} \tag{A.27}$$

References

[1] L.F. Coffin, A note on low cycle fatigue laws, Journal of Materials 6 (2) (1971) 388–402.

[2] J. Weertman, Rate of growth of fatigue cracks calculated from theory of infinitesimal dislocations distributed on a plane, International Journal of Fracture Mechanics 2 (2) (1966) 460–467.

[3] W.G. Fleck, R.B. Anderson, A mechanical model of fatigue crack propagation, in: Proceedings of the Second International Conference on Fracture, Chapman & Hall, Brighton, 1969, pp. 790–802.

[4] G.I. Barenblatt, The mathematical theory of equilibrium cracks in brittle fracture, in: Advances in Applied Mechanics, vol. 7, Academic Press, 1962, pp. 55–129.

[5] D.S. Dugdale, Yielding of steel sheets containing slits, Journal of the Mechanics and Physics of Solids 8 (2) (1960) 100–104.

[6] I.N. Sneddon, The distribution of stress in the neighbourhood of a crack in an elastic solid, Proceedings of the Royal Society of London A 187 (1946) 229–260.

[7] A.P.S. Selvadurai, The penny-shaped crack problem for a finitely deformed incompressible elastic solid, International Journal of Fracture 16 (4) (1980) 327–333.

[8] F.W. Smith, A.S. Kobayash, A.F. Emery, Stress intensity factors for penny-shaped cracks, part I—infinite solid, Journal of Applied Mechanics 34 (4) (1967) 947–952.

[9] Y.M. Tsai, Penny-shaped crack in a transversely isotropic plate of finite thickness, International Journal of Fracture 20 (2) (1982) 81–89.

[10] X. Wang, Elastic t-stress solutions for penny-shaped cracks under tension and bending, Engineering Fracture Mechanics 71 (16–17) (2004) 2283–2298.

[11] A.M. Korsunsky, D.A. Hills, Solution of axisymmetric crack problems using distributed dislocation ring dipoles, Journal of Strain Analysis for Engineering Design 35 (5) (2000) 373–382.

[12] K.S. Parihar, J.V.S.K. Rao, Axisymmetrical stress-distribution in the vicinity of an external crack under general surface loadings, International Journal of Solids and Structures 30 (18) (1993) 2567–2586.

[13] A.E. Green, W. Zerna, Theoretical Elasticity, Oxford, Clarendon Press, 1954.

[14] W.D. Collins, Some axially symmetric stress distributions in elastic solids containing penny-shaped cracks. I. Cracks in an infinite solid and a thick plate, Proceedings of the Royal Society of London, Series A, Mathematical and Physical Sciences 266 (1326) (1962) 359–386.

[15] J.R. Barber, The solution of elasticity problems for the half-space by the method of Green and Collins, Applied Scientific Research 40 (2) (1983) 135–157.

[16] L.M. Keer, A class of non-symmetrical punch and crack problems, Quarterly Journal of Mechanics and Applied Mathematics 17 (4) (1964) 423–436.

[17] L.M. Keer, Stress distribution at the edge of an equilibrium crack, Journal of the Mechanics and Physics of Solids 12 (3) (1964) 149–163.

[18] L.M. Keer, T. Mura, Stationary crack and continuous distributions of dislocations, in: Proceedings of the First International Conference on Fracture, vol. 1, The Japanese Society for Strength and Fracture of Materials, Sendai, Japan, 1965, pp. 99–115.

[19] P.A. Kelly, D. Nowell, Three-dimensional cracks with Dugdale-type plastic zones, International Journal of Fracture 106 (4) (2000) 291–309.

[20] W. Becker, D. Gross, About the penny-shaped Dugdale crack under shear and triaxial loading, ICF 7 (1988) 2289–2299.

[21] W.R. Chen, L.M. Keer, Mixed-mode fatigue-crack propagation of penny-shaped cracks, Journal of Engineering Materials and Technology—Transactions of the ASME 115 (4) (1993) 365–372.

[22] G. Wang, S.F. Li, A penny-shaped cohesive crack model for material damage, Theoretical and Applied Fracture Mechanics 42 (3) (2004) 303–316.

[23] D. Maugis, Contact, Adhesion, and Rupture of Elastic Solids, Springer, Berlin, New York, 2000.

[24] P.H. Jing, T. Khraishi, Analytical solutions for crack tip plastic zone shape using the von Mises and Tresca yield criteria: Effects of crack mode and stress condition, Journal of Mechanics 20 (3) (2004) 199–210.